

# Physicochemical properties and angiogenic potential of whey protein isolate hydrogels modified with heparin or tinzaparin

Zuzanna Pawlak-Likus<sup>a</sup>, Daniel K Baines<sup>b, c</sup>, Nikoleta N. Tavernaraki<sup>d</sup>, Varvara Platania<sup>d</sup>,  
Alan M. Smith<sup>e</sup>, Maria Chatzinikolaidou<sup>d, f\*</sup>, Patrycja Domalik-Pyzik<sup>g</sup>,  
and Timothy E.L. Douglas<sup>b\*</sup>

- a. Department of Biocybernetics and Biomedical Engineering, Faculty of Electrical Engineering, Automatics, Computer Science and Biomedical Engineering, AGH University of Krakow, Al. Mickiewicza 30, 30-059 Kraków, Poland; [zpawlak@agh.edu.pl](mailto:zpawlak@agh.edu.pl)
  - b. School of Engineering Lancaster University, Gillow Avenue, Lancaster LA1 4YW, United Kingdom; [d.baines3@lancaster.ac.uk](mailto:d.baines3@lancaster.ac.uk), [t.douglas@lancaster.ac.uk](mailto:t.douglas@lancaster.ac.uk)
  - c. Biomedical and Life Sciences Lancaster University, Gillow Avenue, Lancaster LA1 4YW, United Kingdom; [d.baines3@lancaster.ac.uk](mailto:d.baines3@lancaster.ac.uk)
  - d. Department of Materials Science and Engineering, University of Crete, GR-70013 Heraklion, Greece; [nikoleta.natalia@gmail.com](mailto:nikoleta.natalia@gmail.com), [plataniavarvara@yahoo.com](mailto:plataniavarvara@yahoo.com), [mchatzin@iesl.forth.gr](mailto:mchatzin@iesl.forth.gr)
  - e. Department of Pharmacy, School of Applied Sciences, University of Huddersfield, Queensgate, Huddersfield HD1 3DH, United Kingdom; [a.m.smith@hud.ac.uk](mailto:a.m.smith@hud.ac.uk)
  - f. Institute of Electronic Structure and Laser, Foundation for Research and Technology Hellas, GR-70013 Heraklion, Greece; [mchatzin@iesl.forth.gr](mailto:mchatzin@iesl.forth.gr)
  - g. Department of Biomaterials and Composites, Faculty of Materials Science and Ceramics, AGH University of Krakow, Al. Mickiewicza 30, 30-059 Kraków, Poland; [pdomalik@agh.edu.pl](mailto:pdomalik@agh.edu.pl)
- \* Corresponding autor: [mchatzin@iesl.forth.gr](mailto:mchatzin@iesl.forth.gr), [t.douglas@lancaster.ac.uk](mailto:t.douglas@lancaster.ac.uk)

## Abstract

A key challenge in tissue engineering is developing functional tissues that can effectively mimic the structure and function of natural tissues. This involves creating scaffolds that support cell proliferation, and differentiation. This research aimed to develop hydrogels as scaffolds that could be utilised in tissue engineering, particularly in applications that require angiogenesis. Whey protein isolate (WPI) has been employed as the main hydrogel component, as WPI hydrogels have been investigated for possible applications in bone tissue engineering. Heparin (HP) and tinzaparin (TP) were selected as additives, as they enhance cellular growth and exhibit anti-inflammatory properties. Nine different compositions were created, each with varying percentages of the additives, a control sample containing pure WPI, and samples with HP or TP at 2.5%, 5%, 7.5%, and 10% concentrations. The mechanical tests showed compressive moduli in the range of 430-620 kPa for the modified hydrogels and indicated that a 5% content of HP or TP is optimal in terms of mechanical characteristics. The highest swelling ratios of approximately 13% and 16%, respectively were noted in both modified groups (TP and HP) at the 7.5% concentration. HP 2.5% demonstrated

the highest cytocompatibility among all HP concentrations, including the WPI control, while TP 10% exhibited greater cytocompatibility than other TP concentrations, also surpassing the WPI control. All hydrogels with additives enhanced cell attachment compared to the WPI control, indicating better cytocompatibility. The morphology visualization of DPSCs indicated no significant differences between the four HP or TP concentrations. TP 10% showed the most promising results in angiogenic differentiation potential tests in vitro, suggesting this composition should be studied further.

Keywords: hydrogel; whey protein; heparin; tinzaparin; tissue engineering

## 1. Introduction

Tissue engineering (TE) combines materials science, biology, and engineering to design environments that facilitate cell attachment and proliferation to substrates, as well as, the formation of complex tissue structures, aiming to create viable replacements for damaged or diseased tissues. The slow growth of blood vessels is a significant challenge in this field, as a proper vascularization is crucial for tissue integration and survival. Hydrogels have gained significant attention in tissue engineering thanks to their superior properties, including their similarities to the extracellular matrix (ECM) of tissues [1]–[3]. Hydrogels were developed by Wichterle and Lim in 1960 [4]. Since then, hydrogels have gained great attention and have been used in various tissue engineering applications, as they can be injectable, implantable or sprayable [5]–[7]. Hydrogels can be utilised in different areas of biomedicine, including wound dressings, drug delivery systems, tissue-engineered implants, and contact lenses. Hydrogels are composed of hydrophilic, cross-linked polymer networks that can retain large amounts of water without losing their 3D structure [2]. Their high water retention and the ease of loading hydrogels with small molecules makes them attractive for TE, as they can contain bioactive molecules like glycosaminoglycans (GAGs) or growth factors (GFs), which facilitate cell growth and differentiation, which are crucial in tissue regeneration [2], [8].

Whey protein isolate (WPI) is a by-product of the dairy industry. Approximately 1.5 million tons of whey protein are produced every year during cheese manufacturing, and this amount is expected to increase because of the growing dairy industry [9]. As WPI is a by-product, it is cheap and available in large quantities [9]. Over 90% of WPI consists of proteins, such as  $\beta$ -lactoglobulin,  $\alpha$ -lactalbumin, bovine serum albumin, and lactoferrin [10]. WPI is known for its high nutritional value and physicochemical properties which facilitate processing using

techniques like foaming, film-forming, emulsifying, water-binding, or gelling [10], [11]. It has found application not only in the food industry, but also in medical and cosmetic sectors [11]. WPI has gained interest as a biomaterial due to its advantageous biological properties, such as antimicrobial bioactivity [9]. Recently, attention has been focused on WPI's ability to form hydrogels, which are sterilizable, show high cytocompatibility, biodegradability, and low toxicity and possess the ability to enhance proliferation and differentiation of osteogenic bone-forming cells [11]–[15].

Heparin (HP) is a heterogenous GAG and a linear polysaccharide that occurs in nature [16]. Since 1935 HP has found its use in clinical applications as a blood anticoagulant [17], [18]. It reduces side effects like inflammatory or coagulant response [8]. Thanks to its highest negative charge density among all the other known biological macromolecules, HP interacts ionically with bioactive molecules like GFs, proteins, and cytokines [2]. Consequently, it is commonly used as coating for implants, especially in a hydrogel form [8]. In addition, HP positively influences bone cells' growth and adhesion [8], [19]. HP plays a key role in many processes such as cell adhesion, proliferation, and binding of proteins that are essential in development, blood clotting, and angiogenesis [20]. Heparin has been shown to enhance angiogenesis primarily by stabilizing and potentiating the activity of growth factors like FGF2, as demonstrated by Manjunathan et al. [21]. Beyond angiogenesis, heparin also contributes to wound healing through its antimicrobial and anti-inflammatory effects. Ahire et al. [22] reported that heparin-capped silver nanoparticle-infused nanofibers enhanced healing while reducing bacterial growth. Similarly, Sayed et al. [23] found that a chitosan/heparin complex improved wound healing in diabetic rats by increasing the collagen content and growth factor expression. Heparin-modified curcumin-loaded nanofibers showed superior wound healing effects compared to unmodified ones [24]. Kohyama et al. [25] further confirmed that heparin synergizes with bFGF to accelerate skin regeneration. Furthermore, Yadav et al. [26] showed that functionalization of liver scaffolds with heparin enhanced angiogenesis and re-endothelialization, underscoring its broader role in vascular tissue engineering.

Tinzaparin (TP) is classified as a low molecular weight HP (LMWH) and is obtained through enzymatic depolymerization of unfractionated HP (UFH) [27]. TP, among all the other LMWHs, has the highest average molecular weight (6,500 Da) [28]. It exhibits the highest anti-IIa activity [28]. Its advantage is that it has more predictable bioavailability and safety than UFH [29]. It also binds less to plasma proteins and has a longer half-life time than

HP [30]. LMWHs have been reported to have a lower risk of inducing osteoporosis [31]. The experiment aimed to investigate, if these advantages can influence the performance of the materials obtained in this study.

Heparinized materials have been developed to promote the therapeutic efficacy of blood-contacting surfaces. Treating catheters, stents and other biomedical devices with HP inhibits blood clotting. A wide range of systems including hydrogels, films, micro and nanoparticle systems and electrospun nanofibrous membranes containing HP have been designed and fabricated to improve biocompatibility [32]. Due to the abundance of functional groups in the structure of HP, heparinized materials can be used in controlled drug and GFs delivery and enhancement of cell adhesion and differentiation. By preventing non-specific protein adsorption and localizing GFs, heparinization promotes cell attachment, proliferation and differentiation on biomaterials [18].

In this research, a new strategy was explored by combining WPI hydrogels with HP or TP to investigate their potential use as scaffolds for TE with enhanced angiogenic potential. Swelling analyses, mechanical tests, and enzymatic degradation analyses were conducted to examine physical properties and differences between control samples and samples containing HP or TP as additives. Infrared spectroscopy (FTIR) and scanning electron microscopy (SEM) techniques were employed to confirm the integration of HP and TP into the WPI hydrogel matrix. Human dental pulp stem cells (hDPSCs) were used for the biological experiments, as they have been previously reported to promote specific angiogenic differentiation markers [33]–[35], making hDPSCs an excellent cellular system to study their angiogenic differentiation potential when cultured on HP and TP-modified WPI-based hydrogels. Cytocompatibility assessments were performed to evaluate the adhesion, viability and growth of hDPSCs seeded on the different types of HP and TP-containing hydrogels. The angiogenic differentiation potential of hDPSCs cultured on the hydrogels was investigated by means of the relative gene expression of specific angiogenic markers.

## 2. Materials and methods

### 2.1. WPI-HP and WPI-TP hydrogel formation

The 40% (w/v) whey protein isolate (WPI) solution was prepared from WPI (Davisco Foods international (Eden Prairie, MN, USA)) and deionized water. Heparin sodium salt (HP)  $M_w \approx 20,000$  g/mol and tinzaparin (TP)  $M_w \approx 8,000$  g/mol, both derived from porcine mucosa,

were supplied by LEO Pharma (Cork, Ireland/Ballerup, Denmark). HP and TP were added separately to 40% WPI solutions to obtain 2.5%, 5%, 7.5%, and 10% HP and TP concentrations. Table 1 presents all the obtained samples with their abbreviations. Samples were left for 1 hour on a vortex to ensure that solutions were well homogenized. Next, solutions were transferred to 2 ml Eppendorf tubes, which were placed in a 70°C water bath for 10 min to induce gelation. The obtained hydrogels were sterilized in an autoclave. Sample groups prepared in this way are described in Figure 1.

**Table 1.** Table with all the obtained samples with their symbols.

Whey protein isolate 40%	Tinzaparin 2.5%	Tinzaparin 5%	Tinzaparin 7.5%	Tinzaparin 10%	Heparin 2.5%	Heparin 5%	Heparin 7.5%	Heparin 10%
WPI	TP25	TP50	TP75	TP100	HP25	HP50	HP75	HP100

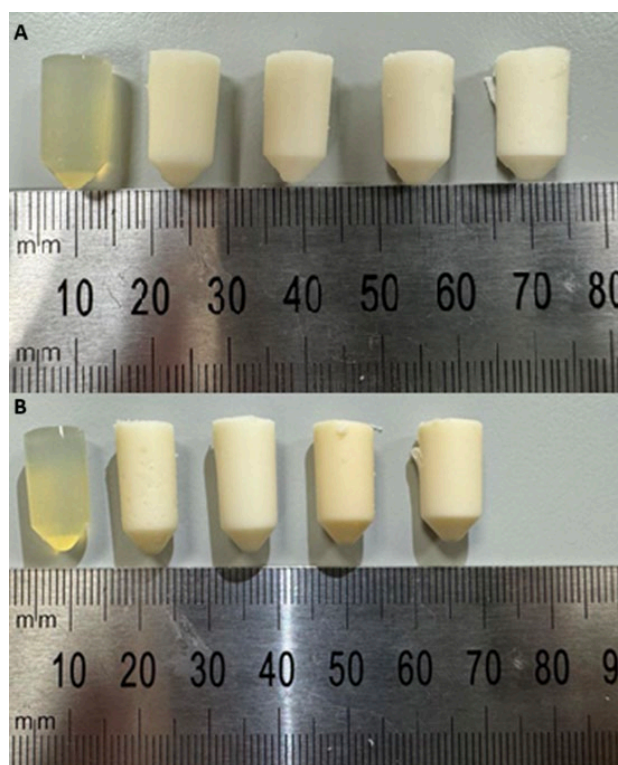


**Fig. 1.** Macroscopic images of the prepared samples, from the left respectively: A) WPI, TP25, TP50, TP75, TP100; B) WPI, HP25, HP50, HP75, HP100.

## 2.2. Fourier Transform Infrared Spectroscopy (FTIR)

To check if HP and TP were correctly incorporated into hydrogels, FTIR analysis was carried out. The device used for tests was an Agilent Cary 630 FTIR. FTIR analyses in attenuated total reflection (ATR) mode were conducted to investigate the chemical bonds in the prepared hydrogels. To conduct the experiment, samples were cut into small pieces, approximately 1 mm in height. After that, each sample was placed on the clean crystal and the measurement started. Samples were tested without prior lyophilisation, to maintain their native structure, in which they would be delivered to the body. Each sample was tested in triplicate.

### 2.3. Swelling ratio

To verify the swelling behavior of hydrogels, 10 samples of each material were incubated in 5 ml PBS solution at 37°C for 5 days. The samples were weighed before and after incubation. Before placing any sample on a scale, the water excess was removed delicately from the surface with a paper towel. The swelling ratio was calculated from the following formula (eq. 1.):

$$S\% = \frac{M_w - M_i}{M_i} \times 100 \quad \text{Eq. 1.}$$

Where  $M_w$  – wet mass,  $M_i$  – initial mass

Results are presented as mean  $\pm$  standard deviation (SD).

### 2.4. Enzymatic degradation

To analyze hydrogel behavior in human body fluids, enzymatic degradation tests were conducted. 10 samples of each material were incubated in 5 ml PBS solution with added protease (2 mg/L) at 37°C for 5 days. The samples were weighed before and after incubation. As in the swelling tests, before placing any sample on the scale, the excess water was removed from the surface with a paper towel. Enzymatic degradation was calculated from the formula (eq. 2.):

$$D\% = \frac{M_a - M_i}{M_i} \times 100 \quad \text{Eq. 2.}$$

Where  $M_a$  – mass after incubation,  $M_i$  – initial mass

Results are presented as mean  $\pm$  standard deviation (SD).

## 2.5. Mechanical analysis

The load-bearing capacity of the hydrogels was evaluated using static compression testing with a maximum strain of 60%. Ten cylindrical samples (1 cm height) were prepared from each material and tested using Zwick Roell machine. Testing parameters included a compression rate of 2 mm/min and a maximum strain of 60%. The compressive stress at 60% strain ( $F$ ) was determined for each sample using the following formula (Eq. 3.):

$$F = \frac{P}{A} \quad \text{Eq. 3.}$$

*Where  $P$  – maximum load at 60% strain,  $A$  – cross-sectional area*

Results are presented as mean  $\pm$  standard deviation (SD).

## 2.6. Protein release

5 samples of each material were placed in 5 ml PBS solution and left in an incubator set at 37°C for 5 days. After 5 days nano-drop tests were conducted, using a UV-VIS method (NanoDrop 2000c, ThermoScientific). Each measurement was repeated 3 times. Results are presented as a mean from all the measurements.

## 2.7. Scanning electron microscopy (SEM) imaging

Samples with 10% HP and TP concentration were chosen on the assumption that the biggest changes in structure would become most apparent at the highest concentrations. Three sample groups were prepared: control sample WPI, HP100, and TP100. A sample from each of the three groups was cut to obtain the middle piece of hydrogel. Each piece was dried overnight before examination with a SEM (JCM-7000 NeoScope™ Benchtop SEM, Jeol).

## 2.8. Cell culture and viability

Cellular viability and behavior assays were conducted utilizing DPSCs. The cells were cultured in alpha-MEM medium supplemented with 15% fetal bovine serum (FBS), 2 mM L-glutamine, 100 µg/mL penicillin/streptomycin, and 2.5 µg/mL amphotericin and incubated in a CO<sub>2</sub> incubator at 37°C. When the cells had reached 80 % - 90 % confluence, they underwent trypsinization and were seeded onto WPI/HP and WPI/TP hydrogels previously sterilized through ultra violet (UV) radiation, for 10 min. Each hydrogel was treated with 50 × 10<sup>3</sup> cells for the proliferation assay and 10 × 10<sup>4</sup> cells for the differentiation assay. Additionally, 200 µl culture medium was added to each hydrogel; this medium was changed every three days. For differentiation assays, DPSCs were exposed to M199 medium, supplemented with 15% FBS, 1% antibiotics/antimycotics (all from Invitrogen), and the following angiogenic supplements: 75 µg/mL endothelial cell growth supplement (ECGS), 50 µg/mL HP (all from Sigma-Aldrich), 50 ng/mL recombinant human (rh) VEGF<sub>165</sub>, (Invitrogen), referred to as angiogenic medium. The angiogenic medium was changed every 2 days for a total period of 21 days.

An AlamarBlue™ viability assay was conducted to assess the cellular viability of the WPI/HP and WPI/TP hydrogels. The hydrogels were treated with DPSCs (n=5). The resazurin-based indicator stains cells, resulting in a red product that can be analyzed photometrically. At days 3 and 5, 200 µl of AlamarBlue™ reagent, diluted in alpha-MEM at a 1:10 ratio, were added to each well and incubated at 37°C for 60 min. Post incubation, 100 µl of the supernatants were transferred to a 96-well plate, and their absorbance was measured at 570 and 600 nm in a Synergy HTX Multi-Mode Microplate Reader (BioTek, Bad Friedrichshall, Germany). After this, the cell-seeded hydrogels were rinsed twice with PBS, and their culture media were renewed.

2.9. Cell adhesion and morphology evaluation via scanning electron microscopy  
SEM was used to examine cell attachment and morphology on the WPI/HP and WPI/TP hydrogels. The assay was conducted with a JEOL JSM-6390 LV SEM, with an accelerating voltage between 15 and 20 kV. DPSCs (50 × 10<sup>3</sup> cells per sample) were seeded onto the hydrogels and incubated in a CO<sub>2</sub> incubator at 37°C for 5 days. On day 5, the hydrogels were rinsed with PBS and fixed using a 4% v/v paraformaldehyde solution, for 15 min. Post fixation, the hydrogels were dehydrated with ethanol with concentrations ranging from 30% to 100% v/v. The hydrogels were dried using hexamethyldisilazane (HMDS) to ensure complete dehydration. This method preserved the structural integrity of hydrogels. Finally,

they were gold coated with a 20 nm thick layer of gold using a sputter coater (Baltec SCD 050).

#### 2.10. Cell migration assay

hDPSCs, in the presence and absence of WPI hydrogels with the addition of HP and TP, were observed under optical microscopy to evaluate their migratory capacity. A cell migration assay was performed following the previously established protocol [36]. hDPSCs were seeded in 12-well plates at a density of  $1 \times 10^6$  cells/well. Once the cells reached 100% confluency, a scratch was introduced to the monolayer using a sterile pipette tip. The cells were then cultured in conditioned angiogenic medium at 37 °C in a 5% CO<sub>2</sub> incubator. Cell migration and wound closure areas were analysed using ImageJ software. All experiments were conducted in triplicates. Data is presented as mean  $\pm$  SD.

#### 2.11. Gene expression analysis by quantitative real time PCR (qPCR)

At days 7 and 21 of differentiation, 1 ml Trizol Reagent was added to the cells for mRNA extraction. The lysate was transferred into tubes and 200  $\mu$ l chloroform were added. After mixing the tubes were left still for 3 min prior to centrifugation for 30 min at 12,000g and 4°C. Approximately 500  $\mu$ l of mRNA were isolated and transferred carefully to new tubes where an equal quantity of isopropanol was added. The tubes were left still for 10 min before being centrifuged for 10 min at 12,000g and 4°C. The supernatants were removed, 1 ml 75% v/v ethanol was added and centrifuged for 5 min at 7500g at 4°C. The supernatants were removed and 15  $\mu$ l RNase free H<sub>2</sub>O was added into every tube. The mRNA concentration and the absorbance ratio 260/280 were measured with Nanodrop before and after the DNase I treatment. For the cDNA synthesis, PrimeScript RT Reagent Kit (Perfect Real Time) (TAKARA, Japan) was used according to the manufacturer's instructions. For the qPCR that was performed in a CFX Connect Bio-Rad quantitative real time PCR system (Bio-Rad, USA), the KAPA SYBR Fast Master Mix (2x) Universal (KapaBiosystems) was used. The primers for the genes examined in this study are presented in Table 2 and include (i) the CD105 or endoglin, which is a receptor for transforming growth factor beta and its expression is upregulated in actively proliferating endothelial cells, (ii) the kinase insert domain receptor (KDR-V) is a gene that encodes the vascular endothelial growth factor receptors (VEGFR), and (iii) the von Willebrand factor (vWF) gene that encodes a glycoprotein involved in hemostasis, by facilitating platelet adhesion to the exposed subendothelium at sites of vascular injury and promoting platelet aggregation [37]. Glyceraldehyde-3-phosphate dehydrogenase

(GAPDH) is a housekeeping gene used as a reference. All assays were performed in triplicate, and the results were expressed as mean  $\pm$  SD.

**Table 2.** Gene symbols and sequences of the forward and reverse primers.

Gene symbol	Forward (5'-3')	Reverse (5'-3')
<i>GAPDH</i>	AGC CAC ATG GCT CAG ACA C	GCC CAA TAC GAC CAA ATC C
<i>CD105</i>	AGT CTT GCA GAA ACA GTC CA	TGG ACT TCA AGG ATG GCA TT
<i>KDR-V</i>	CAG CTC ACA GTC CTA GAG CG	AGA TGC CGT GCA TGA GAC TT
<i>vWF</i>	GCT GAC ACC AGA AAA GTG CC	GTC CTG GAA GAC GTC ACT GG

### 2.12. Tube formation assay

hDPSCs, in the presence and absence of WPI hydrogels with HP and TP, were observed under optical microscopy to evaluate the modulation of their tube formation potential. Tube formation assay was performed following a previously established protocol [38]. For the tube formation assay, hDPSCs were seeded in 24-well plates at a density of  $5 \times 1000$  cells/well, and maintained in angiogenic medium. Tube-like structures were evaluated after 12 and 24 h of incubation at 37 °C in a 5% CO<sub>2</sub> environment. All experiments were conducted in triplicates. Data is presented as mean  $\pm$  SD.

### 2.13. Statistical analysis

Statistical analysis was carried out using an ANOVA t-test in GraphPad Prism version 8 software to assess the significance of differences among various hydrogel compositions and the control at different experimental time periods. A p-value (\*) less than 0.05 was considered significant, \*\*p < 0.01, \*\*\*p < 0.001, \*\*\*\*p < 0.0001, compared to the WPI control hydrogel at the corresponding time point.

## 3. Results and discussion

### 3.1. FTIR

Figure 2 presents the results of the FTIR-ATR spectroscopy; a control sample (WPI), the additive in powder form (HP or TP) and hydrogels containing the additive (HP or TP) with

concentrations of 2.5%, 5%, 7.5%, and 10%. It can be seen that the addition of HP and TP flattened the peak around  $3200\text{cm}^{-1}$ . A peak around  $1000\text{cm}^{-1}$ , a main carbohydrate band (blue color), and sulphate stretch band (orange color) at around  $1200\text{cm}^{-1}$ , visible on pure HP and TP powders, can be also seen on WPI hydrogels with HP and TP additives, and they become more intense with increasing additive concentration, which suggests that the additives were successfully incorporated into hydrogels [39], [40].

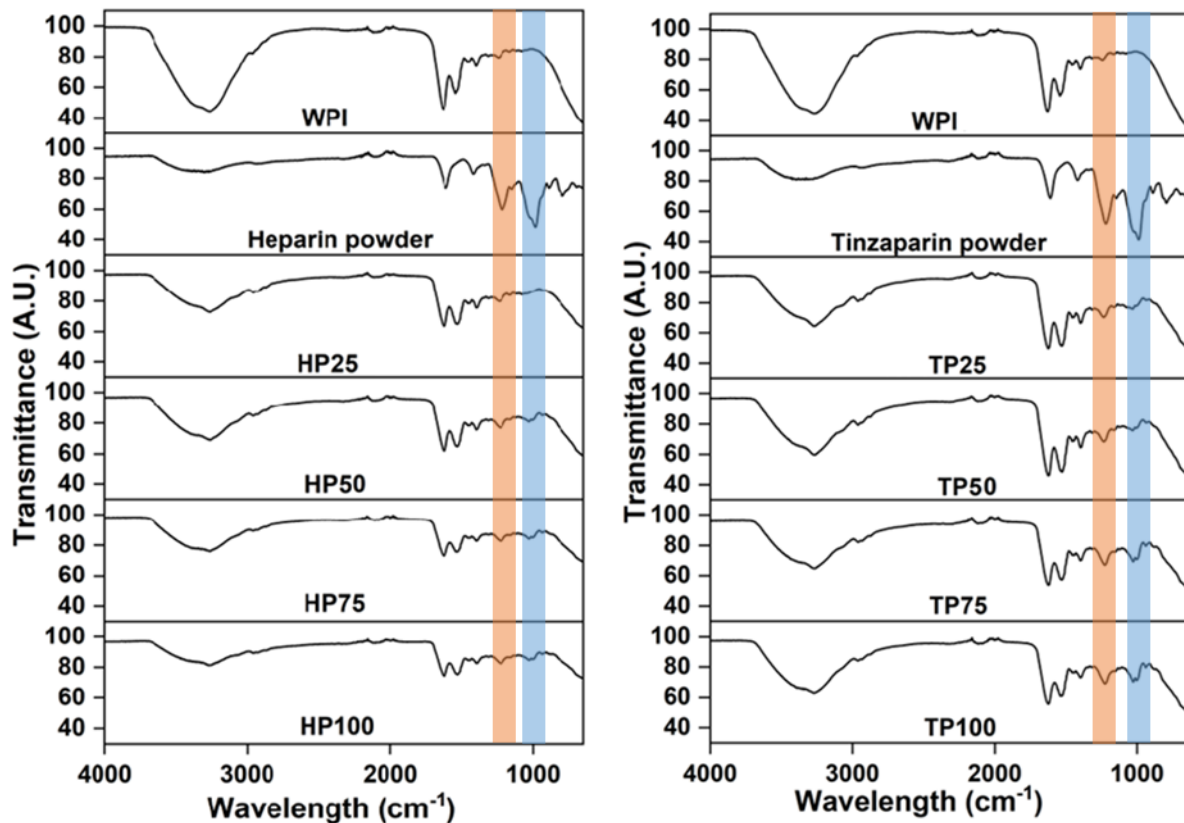


**Fig. 2.** Results of FTIR analysis with highlighted characteristic heparin peaks. The orange color represents a sulphate stretch band and the blue color represents a main carbohydrate band.

### 3.2. Swelling

The results of the swelling assay can be observed in Figure 3A. The results demonstrate the swelling ratio of each hydrogel sample group, calculated by eq. 1. Both HP and TP are highly hydrophilic molecules due to the presence of sulphate groups. Sulphate groups are highly negatively charged, and due to electrostatic repulsion can increase in osmotic pressure within the hydrogel and the result is a hydrogel with a higher swelling potential. Therefore, it was expected that the swelling ratio would be higher in the HP and TP

sample groups when compared to the control sample [18]. However, not all samples followed the expected trend. For example, the TP25 variables demonstrated a lower swelling ratio than the WPI control sample. Additionally, the HP25 group had only slightly higher swelling ratio than the WPI control. A potential explanation could be that the small amount of additives like HP and TP does not exert a great influence on swelling. This would be because at lower HP and TP concentration there are more available positively charged regions on the WPI for the HP and TP to electrostatically bind to. This results in ionic crosslinking and a tighter hydrogel network and a lower swelling ratio. As more HP and TP is introduced to higher concentrations, there is less WPI to interact with and more negatively charged hydrophilic sulphate groups, causing the osmotic pressure, resulting in higher swelling.

The highest swelling ratio is for the 7.5% concentration for both HP and TP, which suggests that this concentration is the best choice when preparing hydrogels with HP or TP for tissue engineering. Biomaterials possessing a high swelling ratio are desirable in tissue engineering [41]. Hydrogels are very often enriched with additives that can induce the desired process. Both synthetic (e.g. metal ions) and natural (e.g. GFs) compounds can be used [41], [42]. The highest swelling ratio from all the examined samples was for HP75, and was almost 4 times higher than the swelling ratio of the control sample. Samples of 10% concentration showed a lower swelling ratio than the 7.5% samples, which could suggest a higher degree of crosslinking, went too high, and there is less space for water to bind [43][44]–[47]. Additionally, the mass loss for the 10% variables could be the result of degradation with weakening structural integrity past a certain HP and TP concentration. However, any potential discussion surrounding the binding between WPI and HP TP is currently speculation and requires further investigations.

### 3.3. Enzymatic degradation

The results for the enzymatic degradation assay can be observed in figure 3B. Any degradation was determined by change in mass calculated using eq. 2. The swelling % of HP and TP-containing samples is higher than both the WPI control variables. A possible explanation for this process could be that enzymes break down the bonding between molecules, which in turn allows more water to bind into the hydrogel before it is degraded. Additionally, the proteases used in the investigation cleave peptide bonds. An increase in HP and TP reduces the number of available peptide bonds for cleavage while maintaining the

electrostatic repulsion discussed in the swelling section. The mass change ratio for HP25 and HP50 samples is lower than for the control sample. Changes in a polymer mesh size can affect the degradation rate of hydrogels, as a smaller mesh size can be less accessible for larger molecules such as enzymes, decreasing the hydrogel degradation rate [2][48]. This could be the explanation for the results of samples HP25 and HP50. However, such discussion must remain speculative. The results show that with manipulating the concentration of added HP, it is possible to change the degradation rate of WPI hydrogels, either decrease or increase it. The result for TP100 is similar to that of the control sample. Adding TP at a concentration between 2.5% and 10% to WPI hydrogels increases the mass change ratio for hydrogels compared to the control sample.

Comparing swelling and enzymatic degradation analyses in HP samples, it can be seen that lower concentrations (HP25 and HP50) do not impact these properties of hydrogels as much as higher concentrations (HP75 and HP100) do. This can be explained through the fact that the addition of low HP concentrations only slightly affects the polymer mesh structure, and consequently, their swelling and enzymatic degradation properties. Higher HP concentrations may enhance binding of water molecules, which may favor enzymatic degradation. The opposite trend was observed in samples with TP, as the highest mass change is observed for TP50, while lower or higher concentrations of TP decrease the mass change. Notably, the swelling behavior does not correlate with the enzymatic degradation behaviour, which implies that other mechanisms may be involved in these processes. TP50 exhibited the highest mass change, which may form breakdown of the hydrogel network that increases enzyme accessibility. Higher concentrations of TP may result in higher ionic interactions between TP and WPI, which have an impact on stabilizing the hydrogel's structure.

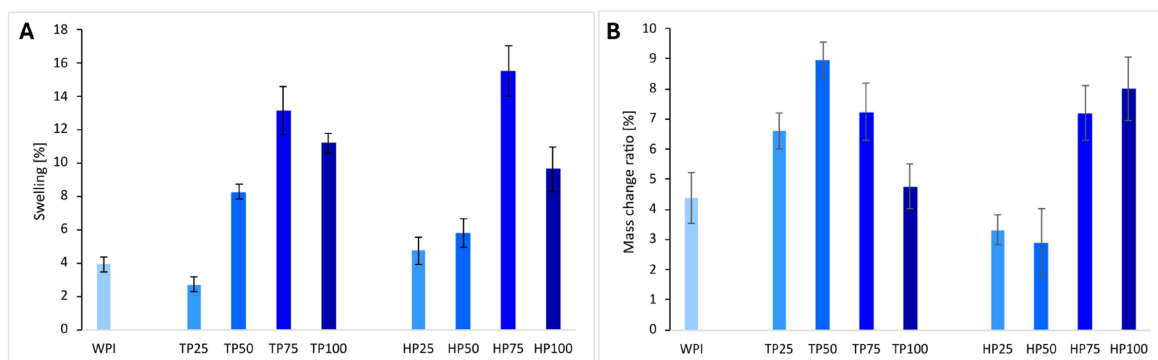


**Fig. 3.** Diagrams showing A) the average swelling ratio [%] and B) the enzymatic degradation expressed as average mass change ratio [%] after 5 days of incubation with standard deviation poles for each material [n=10].

### 3.4. Mechanical analysis

Figure 4 shows the average compressive stress at 60% strain for each sample group. The control sample shows the highest compressive stress at 60% strain, and as predicted, the additives lower the compressive stress values. The explanation could be that HP and TP increase hydrogel porosity, which leads to lower mechanical properties [3]. The trend of lower mechanical properties at 2.5%, an increase at 5%, and a subsequent decrease at higher concentrations is consistent for both additives. Both TP50 and HP50 showed the best results among the samples with additives, suggesting that a 5% additive concentration is optimal for achieving the best mechanical properties. In samples with added TP, there are no visible differences between the concentrations, whereas in samples with HP, a notable difference is observed between HP50 and HP100.

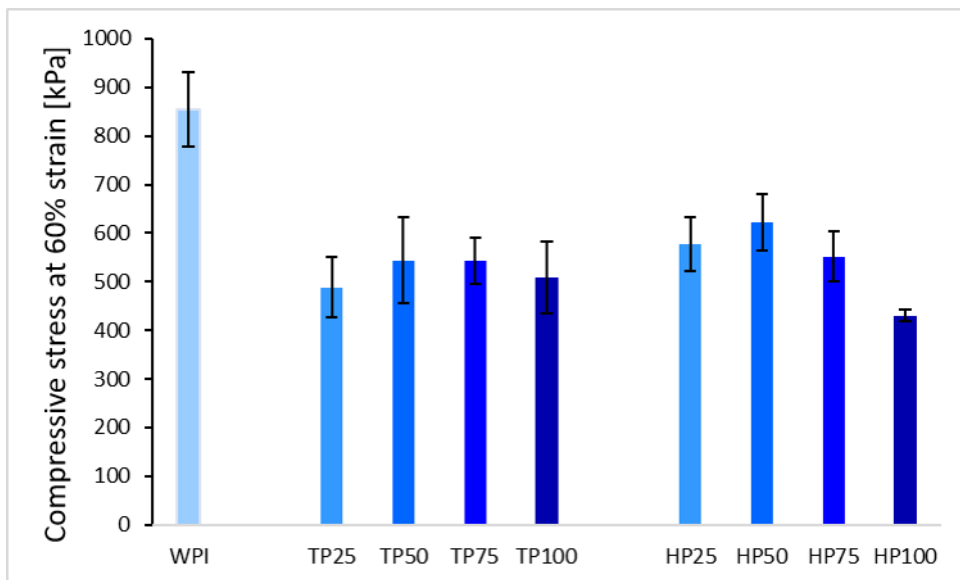


**Fig. 4.** Diagram showing average compressive stress at 60% strain [kPa] with standard deviation poles for each material [n=10].

### 3.5. Protein release

Figure 5 shows the protein release measured with a UV-VIS NanoDrop equipment. In both pictures, the whole measured spectrum is shown on the left, while on the right, a specific wavelength range presents a difference in protein release from each material. It is apparent that the control sample without any additives showed the highest absorbance, demonstrating that the protein release was the highest from these samples. Samples with the addition of HP and TP showed lower values, which could suggest that less protein is released. This may conceivably be due to strong bonds between protein in WPI and TP or HP. If the mesh size is smaller and crosslinking is higher, the release of protein may be hindered [2], [48].

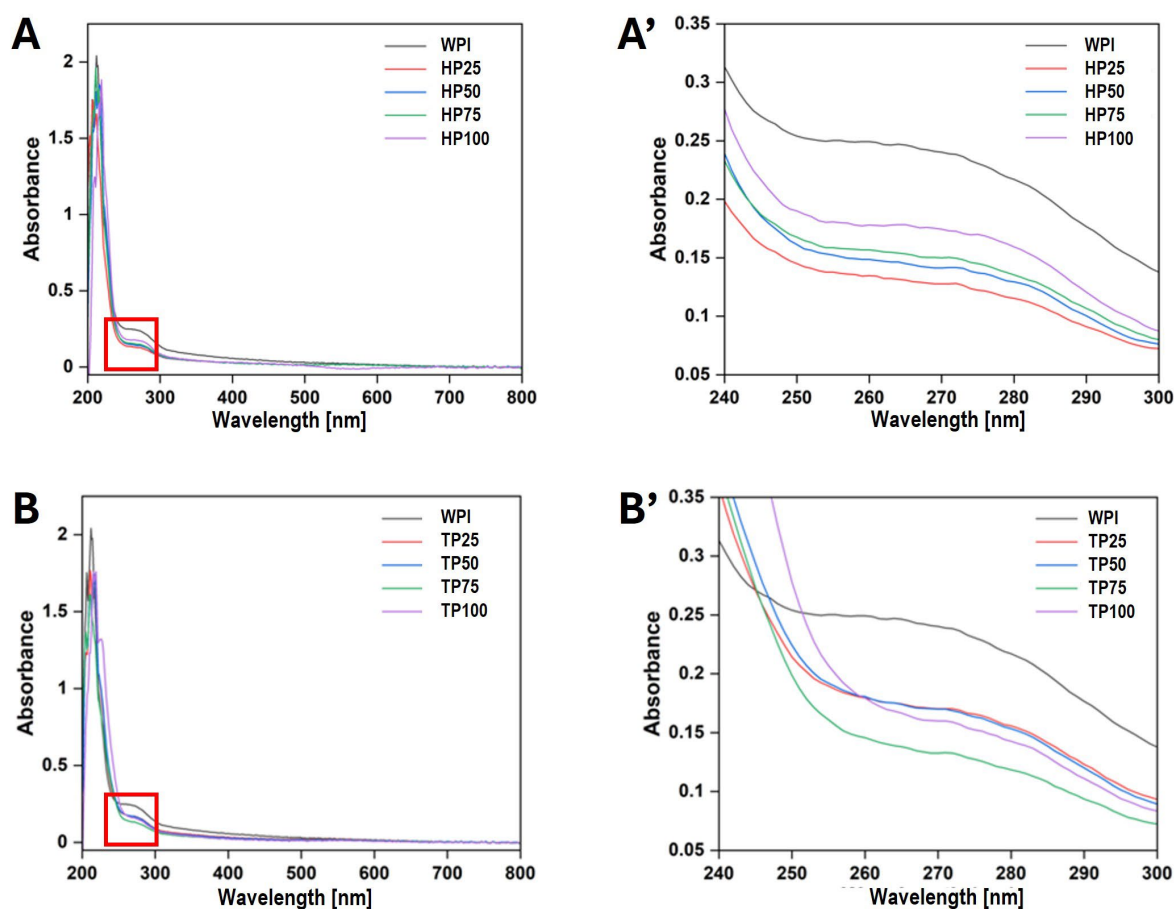


**Fig. 5.** Results of photometric measurements of the protein release profile for WPI and WPI with A), A') HP and B), B') TP at different concentrations: A), B) the absorbance across the entire wavelength range; B) a detailed view of the boxed region (240-300 nm).

### 3.6. SEM imaging

SEM analysis (Fig. 6) revealed clear differences in terms of the microstructure and morphology of the hydrogels with and without the additives. However, HP and TP-modified

samples were similar. Both are characterized by visibly round-shaped substructures, while the WPI hydrogel appears smoother. It indicates that hydrogels containing HP and TP are well-bonded and have more porous microstructure in the dry state, which is a desirable property in TE [3]. Porosity provides space for cells to migrate and proliferate through biomaterial, which leads to forming a new tissue, while the biomaterial is degraded. However, it should be noted that the structure in the dry state is not necessarily representative of the structure in the wet state. In the absence of further data, such discussion must remain speculative.

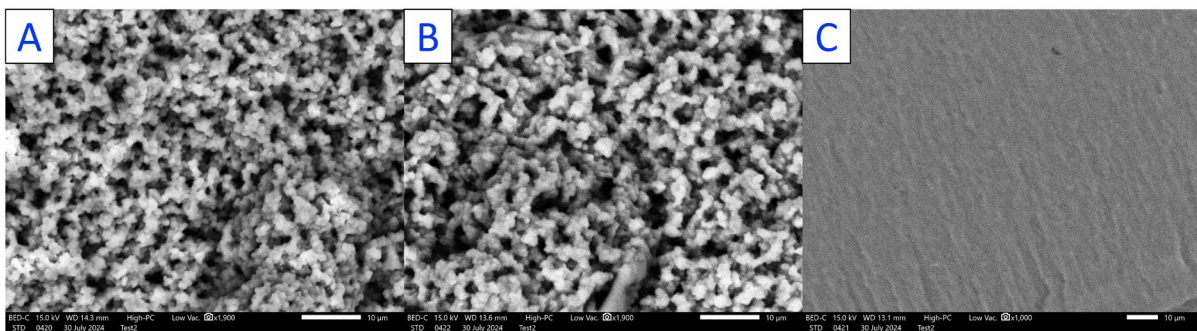


**Fig. 6.** SEM images of the hydrogels: A) HP100, B) TP100, and C) WPI; scale bar 10  $\mu\text{m}$ .

### 3.7. Cytocompatibility of the hydrogels

*In vitro* analysis with DPSCs was conducted to determine the cytocompatibility of WPI with HP and WPI with TP hydrogel samples. An AlamarBlue<sup>TM</sup> cell viability assay was utilised to assess the cytocompatibility on days 3 and 5 in culture (Fig.7A). No significant differences were evident among the different sample groups containing additives compared to the WPI control. However, for the WPI hydrogels containing HP, as the concentration of HP increases, the cytocompatibility levels slightly decrease. On day 5, the HP25 sample exhibited the highest cell viability values compared to all other concentrations, including the WPI control; however, the differences were not statistically significant. The opposite trend was observed for the WPI with TP variables. TP100 exhibited higher absorbance values among the other WPI with TP variables including the WPI control, on day 5. These molecular size optimized LMWHs or ultra low molecular weight HPs (ULMWHs) have shown great potential in clinical applications as drugs with improved therapeutic effects and low toxicity when compared with large UFHs [49]. No obvious correlation with swelling (Fig. 3) and mechanical testing results (Fig. 4) was observed.

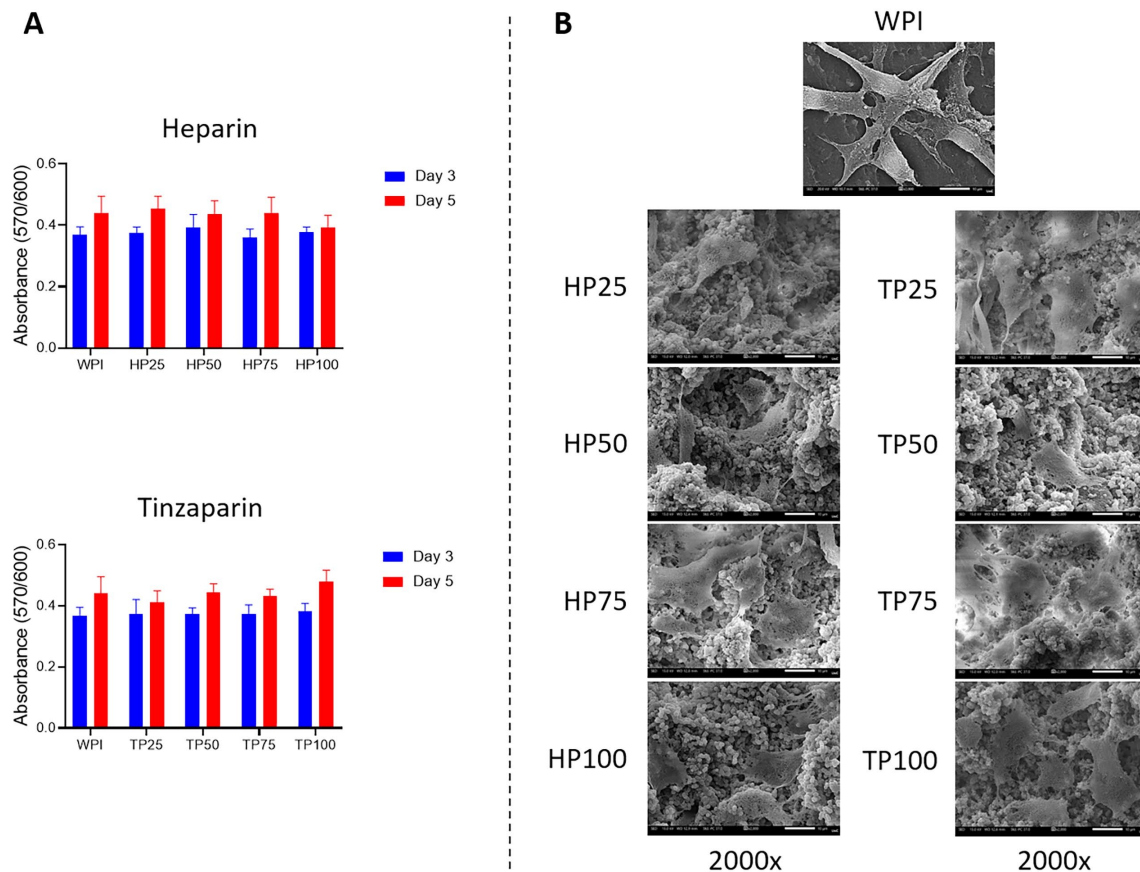


**Fig. 7.** A) Cell viability and proliferation of DPSCs seeded on WPI with HP and WPI with TP hydrogels. Absorbance values were taken at days 3 and 5. Each bar represents the mean  $\pm$  SD of  $n=5$ . B) SEM images demonstrating the cellular morphology of DPSCs on WPI with HP (left) and WPI with TP (right) hydrogels (B). Images were taken in 2000x magnification after 5 days in culture. The scale bars represent 10  $\mu\text{m}$ .

### 3.8. Cell adhesion and morphology evaluation

The cells change their shape and morphology to adhere onto the biomaterial surface once they come into contact with it. The progress of cell adhesion and spreading consists of cell attachment, filopodial growth, cytoplasmic webbing, flattening of the cell mass and the ruffling of peripheral cytoplasm [50]. Therefore, cell adhesion has been widely used to investigate the cell behaviour on biomaterials. In this study, the adhesion of DPSCs was assessed through SEM imaging (2000 $\times$  magnification) after 5 days in culture (Fig. 7B). DPSCs cultured on the WPI with HP and WPI with TP hydrogel compositions demonstrated robust attachment to the hydrogels. By day 5, dense layers of cells were observed, along with prominent cell–cell interactions, which are likely to support tissue formation. All hydrogel

types showed stronger cell attachment compared to the WPI control, indicating enhanced cytocompatibility and cellular integration onto the hydrogels. Similar to the viability assessment, the set of SEM images did not reveal any substantial differences between the various concentrations, with the exception of the control. Cells cultured on WPI control hydrogel appeared more rounded and showed limited spreading. This is in line with previous studies reporting that tissue culture surfaces coated with GAGs such as HP support greater proliferation of MSCs [51], [52]. Additionally, HP-functionalized hydrogels and heparinized nanoparticles have also been developed to support the viability and differentiation of hMSCs [53], [54]. No obvious correlation with swelling (Fig. 3) and mechanical testing results (Fig. 4) was observed.

### 3.9. Wound healing assay

The scratch test, also known as wound healing assay, is a method used to evaluate the angiogenic potential of cells, as cell migration is a key parameter in the formation of new blood vessels. After a scratch was made on an hDPSCs monolayer, optical microscopy images were taken at 0, 8, 16, 24, and 32 h (Figure 8A). All of the samples showed complete wound closure at the final time point. At 24 h the samples showed the same significant difference (Figure 8B). Significant differences were not observed between the control, TP25 and HP100 at 16 h, while all the other samples showed significant differences. These samples exhibit the most similar behaviour in comparison to the control sample, suggesting their effect on the natural behaviour. The lengths (gaps) at 24 h were the smallest for TP25 and HP100. TP25 and HP100 exhibited the most pronounced cell migration, suggesting enhanced angiogenic potential compared to other conditions.

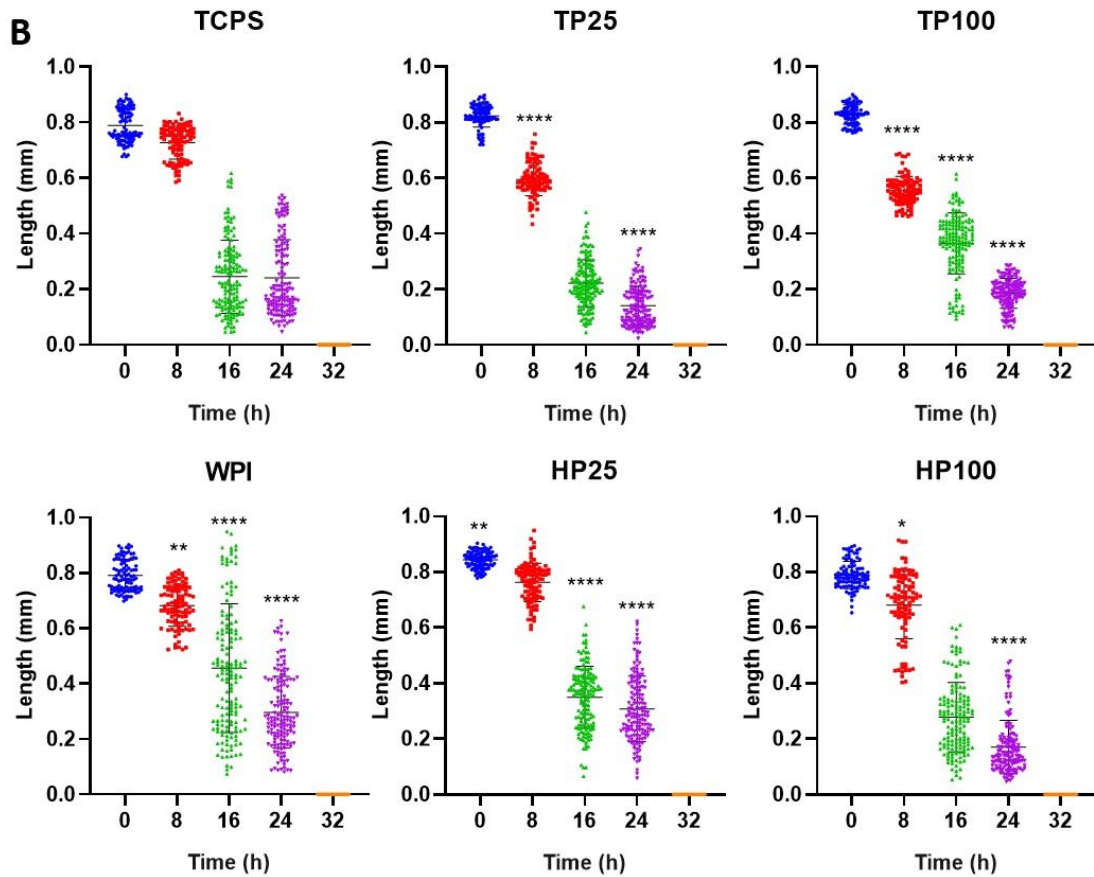
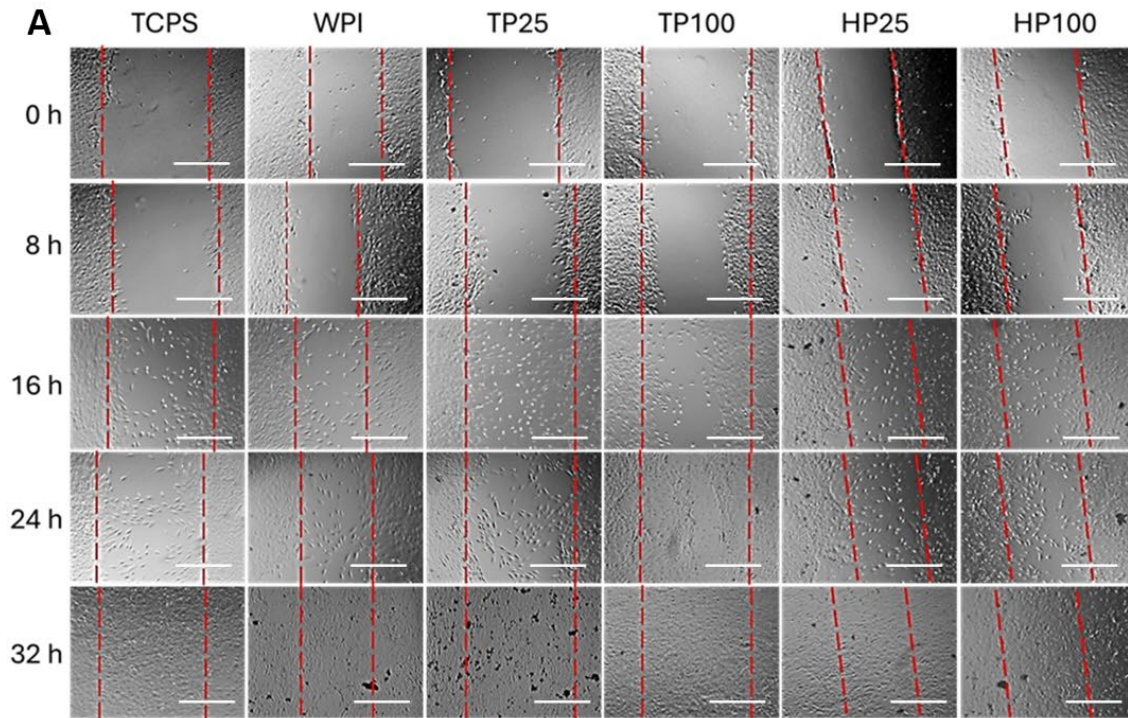


**Fig. 8.** Representative optical microscopy images (A) and quantification of the length (gap closure) (B) of the cell migration assay taken at 0, 8, 16, 24, and 32 h. From the left: TCPS; WPI; TP25; TP100; HP25; HP100. Dashed lines (in red) were added to depict the scratch (gap). Scale bars represent 00  $\mu\text{m}$ . Significant differences were calculated between the tissue culture treated polystyrene (TCPS) control and each of the samples. Each graph represents the mean  $\pm$  SD of at least  $n=100$  (\* $p<0.05$ , \*\* $p<0.01$ , \*\*\*\* $p<0.0001$ , denotes a statistically significant difference compared to the TCPS control).

### 3.10. Evaluation of the angiogenic differentiation potential of the hDPSCs cultured on hydrogels

hDPSCs hold significant promise for promoting vasculogenesis and angiogenesis [33], as they are capable of differentiating into endothelial cells in vitro [34], [35]. This unique capability makes hDPSCs highly suitable for exploring the angiogenic differentiation processes for tissue engineering applications. The evaluation of the relative gene expression at days 7 and 21 for the WPI with HP and WPI with TP containing hydrogels provided critical insights into the angiogenic differentiation potential and maturation of DPSCs. The relative gene expression levels of CD105, KDR-V and vWF at these time points were examined (Fig. 9). The lowest (TP25, HP25) and highest (TP100, HP100) concentrations were selected for this study. The assessment of the lowest and highest concentrations allows for a comparison between minimal and maximal dose effects, providing insight into both the supportive and potentially inhibitory roles of HP and TP on angiogenic differentiation.

For the HP-containing hydrogels on day 7, HP100 exhibited significantly higher levels of CD105 expression compared to the control WPI, suggesting enhanced angiogenic response, while HP25 demonstrated lower CD105 expression than the control. By day 21, all hydrogels showed a decrease except HP25, which could be linked to the higher CD105 expression observed earlier on day 7.

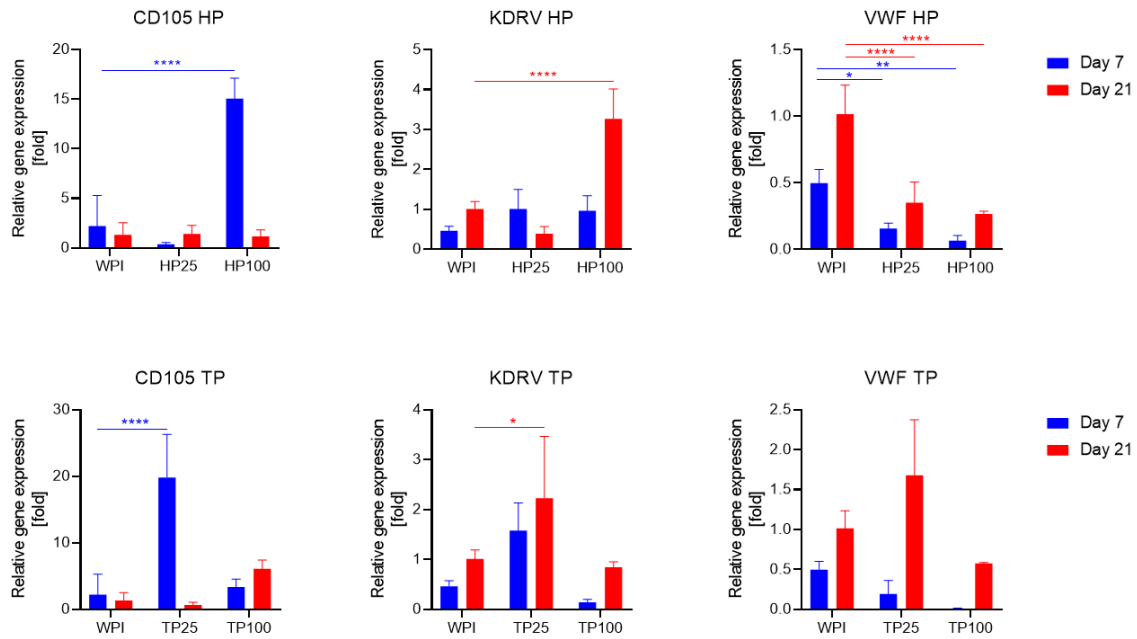


**Fig. 9.** Relative expression levels of the genes CD105, KDR-V, vWF after 7 and 21 days in culture conditions for the heparin-containing hydrogels (upper panel) and tinzaparin-containing hydrogels (lower panel). Each bar represents the mean  $\pm$  SD of  $n=3$ . Bars that are not visible indicate expression levels  $<1$ -fold (\* $p<0.05$ , \*\* $p<0.01$ , \*\*\*\* $p<0.0001$ , denotes a statistically significant difference compared to the WPI control). The values that are not visible represent a relative gene expression  $<1$ .

On day 7, HP25 and HP100 had approximately similar KDR-V levels, which were higher than WPI. On day 21, a distinct trend emerged, HP25 experienced decreased KDR-V levels compared to day 7, while WPI and HP100 samples increased their values, with the latter presenting significantly higher values than the control. This rise might indicate a prolonged retention of VEGFR-2 or delayed activation respectively. The VEGFR-2 signalling pathway, the most critical ligand-receptor pair within the VEGF system, activates networks that drive endothelial cell proliferation, migration, survival, and the formation of new blood vessels, which is essential for angiogenesis. Moreover, the presence of VEGFR2 also integrates mechanical and chemical cues, contributing to enhanced endothelial differentiation [55].

On day 7, WPI showed the highest vWF expression, indicating strong angiogenic activation. HP25 and HP100 showed lower vWF expression values, which suggests that HP may have initially hindered angiogenic activation or impaired early vWF production. This could also be attributed to HP's role in modulating hemostasis [56]. VWF is a key factor to primary

hemostasis, facilitating platelet adhesion and aggregation at sites of vascular injury. HP, incorporated into these hydrogels, acts as a potent anticoagulant by inhibiting thrombin and Factor Xa activity [57]. This anticoagulant environment created by HP could suppress early vWF expression as the hydrogels establish a microenvironment that activates anticoagulation. On day 21, WPI presented the highest values. However, as differentiation progresses, vWF expression increases for HP25 and HP100, potentially signalling the cell transition toward a more mature endothelial phenotype. Significant differences were not observed. Such trends show that while WPI initially promoted higher vWF expression, HP may provide a late-stage boost. According to a previous study [58], PLLA/HP scaffolds have been reported to support angiogenic differentiation over time. Extended experiments demonstrate the sustained expression of angiogenic markers such as CD31 and vWF beyond one week. The observed persistence and progression of these markers, suggests the scaffolds' ability to induce a sustained angiogenic commitment while maintaining the biological functionality of released HP.

In general, HPs facilitate the binding of many proteins to high-affinity receptors on cells, particularly within the endothelium [38], [59]. The gene expression profile of the DPSCs stimulated in the presence of HP can be explained through factors such as VEGF<sub>165</sub> and FGF-2, which normally associate with heparan sugars on cell surfaces to form ligand:sugar:receptor complexes that induce proliferative signals. It is also well described in the literature that VEGF<sub>165</sub> affinity-selected sugars have been shown to exert pro-angiogenic effects on endothelial cells [60].

For the TP-containing hydrogels on day 7, TP25 exhibited significantly higher levels of CD105 expression compared to the control WPI, suggesting enhanced angiogenic response. TP100 demonstrated lower CD105 expression but higher than the control. By day 21, all hydrogels showed a decrease except TP100, which maintained higher CD105 levels than the control, which could be translated to sustained angiogenic stimulation.

WPI control hydrogels and TP25 exhibited the highest KDR-V expression on day 7 with TP25 having higher KDR-V levels compared to WPI. TP100 had the lowest KDR-V expression on day 7, suggesting that higher TP concentrations may have inhibitory effects on the VEGFR-2 pathway. By day 21, all samples displayed increased expression values. However, TP25 showed significantly higher values than the control.

On day 7, WPI showed the highest vWF expression, indicating strong angiogenic activation. On day 21, all samples showed increased vWF expression. TP25 had the highest vWF values, which suggests that TP may have initially hindered angiogenic activation or impaired early vWF production. Such trends show that while WPI initially promoted higher vWF expression, TP may cause a late-stage increase in vWF, suggesting delayed but extended angiogenic activity. No significant differences were observed.

As a consequence of the lower mean molecular weight of the HP fragments, it is possible that the LMWHs used in this study might prevent the binding of GFs to their receptor on endothelial cells and thus inhibit their functions [61]. Our results are in line with those of other studies that have explored the effects of HPs on angiogenesis in different experimental *in vivo* and *in vitro* models. In an animal model of angiogenesis, it has been shown that FGF-2- and VEGF<sup>165</sup>-induced angiogenesis is more suppressed by a LMWH, or HPs enriched in 2.5 kDa and 5.0 kDa species, than by high molecular weight HPs [62], [63]. Similarly, in an *in vitro* model of angiogenesis in human umbilical vein endothelial cells, LMWH in the range of 3–6 kDa significantly inhibited FGF-2- and VEGF-induced angiogenesis, whereas no inhibition was observed with UFH, tetrasaccharide, pentasaccharide and octasaccharide [64].

Overall, the results demonstrate that both HP- and TP-containing WPI hydrogels affected the cytocompatibility and the angiogenic potential of hDPSCs, with variations observed depending on the concentration of HP and TP. SEM imaging and cell viability assays confirmed robust cell attachment and viability across all hydrogel types, with HP25 and TP100 showing the highest cytocompatibility by day 5, however, the differences were not statistically significant. Gene expression analysis revealed that higher concentrations of HP and TP (HP100, TP100) supported the prolonged expression of the markers CD105, KDR-V, vWF, indicating sustained angiogenic stimulation. These findings highlight the potential of tailored HP and TP concentrations in hydrogels to optimize the angiogenic differentiation potential in tissue engineering applications.

### 3.11. Tube formation assay

Tube formation assay is an effective method for evaluation of the angiogenic potential of biomaterials. Figure 10 presents the results of the assay with images taken at 12 and 24 h. In the control samples, cells appear more aligned in linear arrangements, whereas TP25 and

HP100 exhibit the most distinct tube-like structures. TP100 and HP25 also show some circular or rounded formations, but these are less prominent.

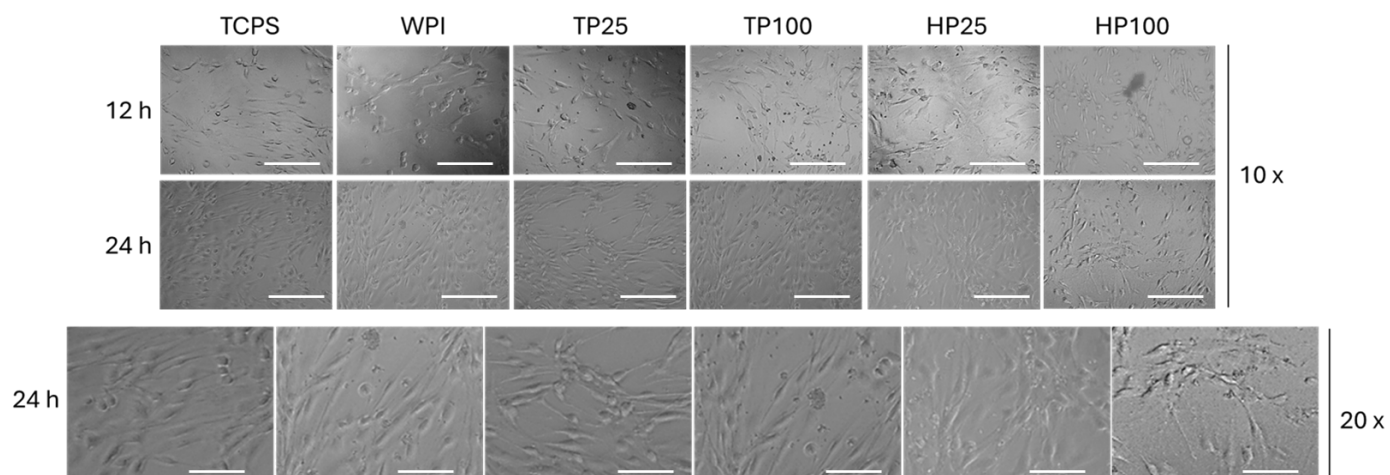


**Fig. 10.** Optical microscopy images depicting the tube formation taken after 12, and 24 h. From the left: TCPS; WPI; TP25; TP100; HP25; HP100. Scale bars represent 100  $\mu\text{m}$  at 10x magnification (upper panel), and 50  $\mu\text{m}$  at 20x magnification (lower panel).

#### 4. Conclusions and Outlook

The objective of this research was to study WPI hydrogels synthesized with 2.5%, 5%, 7.5%, and 10% concentrations of HP or TP. FTIR and SEM analyses confirmed successful incorporation of both additives into the hydrogels. Mechanical tests showed a similar trend for both, with the 5% concentration yielding the highest results. The 7.5% concentration displayed the greatest swelling properties, though the difference between TP75 and TP100 was smaller than between HP75 and HP100. None of the samples were cytotoxic, although increased HP content slightly decreased cytocompatibility. After 5 days, TP100 and HP25 displayed higher cytocompatibility compared to the control. SEM imaging revealed that hydrogels with HP or TP displayed better cell attachment than the WPI control, with no significant differences among the concentrations. Gene expression analysis by quantitative PCR revealed that HP100 and TP25 exhibited the highest angiogenic potential in vitro. These samples showed the highest KDR-V expression after 21 days and the highest CD105 levels after 7 days. Among all tested samples, TP25 demonstrated the strongest vWF expression. The results of the scratch and tube formation assays are consistent with the PCR data, as TP25 and HP100 also showed the most pronounced proangiogenic activity in these functional tests. The obtained hydrogels had a positive impact on angiogenic markers, and in the previous

works they were reported to enhance osteogenesis. Taking those facts into consideration, WPI hydrogels with the addition of HP and TP may find use as a material promoting angiogenesis. The sample containing 2.5% TP showed the best properties overall among all the other samples, and is recommended for further evaluation, which should focus on additional angiogenic markers and other cellular responses in endothelial cells in vitro.

#### Abbreviations:

WPI - whey protein isolate;

HP - heparin;

TP - tinzaparin;

TE - tissue engineering;

GFs - growth factors;

GAGs - glycosaminoglycans;

TCPS - tissue culture treated polystyrene;

ECM - extracellular matrix;

hDPSCs - Human dental pulp stem cells.

#### CRedit authorship contribution statement

Zuzanna Pawlak-Likus: Writing – original draft, Investigation, Data curation; Daniel K Baines: Investigation; Nikoleta N. Tavernaraki: Methodology, Investigation, Data curation, Writing – review & editing; Varvara Platania: Methodology, Investigation, Data curation, Writing – review & editing; Alan M. Smith: Methodology, Writing – review & editing; Maria Chatzinikolaidou: Methodology, Writing – review & editing, Conceptualization, Supervision, Funding acquisition; Patrycja Domalik-Pyzik: Methodology, Writing – review & editing, Conceptualization, Supervision; Timothy E.L. Douglas: Methodology, Writing – review & editing, Conceptualization, Supervision, Funding acquisition

## Declaration of competing interest

The authors have no competing interests to declare.

## Acknowledgements

This study was supported by the Program “Excellence Initiative – Research University” for the AGH University of Krakow (10429), the Hellenic Foundation for Research and Innovation (grant number HFRI-FM17-1999), and the Faculty of Science and Technology, Lancaster University for a doctoral stipend for Daniel Baines.

## Data availability

Data will be made available on request.

## References

- [1] P. Zarrintaj *et al.*, “Biopolymer-based composites for tissue engineering applications: A basis for future opportunities,” *Compos. Part B Eng.*, vol. 258, no. November 2022, p. 110701, 2023, doi: 10.1016/j.compositesb.2023.110701.
- [2] P. M. Kharkar, K. L. Kiick, and A. M. Kloxin, “Designing degradable hydrogels for orthogonal control of cell microenvironments,” *Chem. Soc. Rev.*, vol. 42, no. 17, pp. 7335–7372, 2013, doi: 10.1039/c3cs60040h.
- [3] M. U. A. Khan, M. A. Aslam, M. F. Bin Abdullah, A. Hasan, S. A. Shah, and G. M. Stojanović, “Recent perspective of polymeric biomaterial in tissue engineering– a review,” *Mater. Today Chem.*, vol. 34, no. November, 2023, doi: 10.1016/j.mtchem.2023.101818.
- [4] O. Wichterle and D. Lim, “Hydrophilic Gels for Biological Use,” *Nature*, vol. 185, pp. 117–118, 1960, doi: <https://doi.org/10.1038/185117a0>.
- [5] M. Y. Yingying Liao, Luoyijun Xie, Jiahui Ye, Tong Chen, Tong Huang, Leilei Shi, “Sprayable hydrogel for biomedical applications,” *Biomater. Sci.*, no. 11, pp. 2759–

2771, 2022.

- [6] M. Liu *et al.*, “Injectable hydrogels for cartilage and bone tissue engineering,” *Bone Res.*, vol. 5, no. November 2016, 2017, doi: 10.1038/boneres.2017.14.
- [7] X. Xue, Y. Hu, Y. Deng, and J. Su, “Recent Advances in Design of Functional Biocompatible Hydrogels for Bone Tissue Engineering,” *Adv. Funct. Mater.*, vol. 31, no. 19, pp. 1–20, 2021, doi: 10.1002/adfm.202009432.
- [8] D. Facchetti *et al.*, “Heparin enriched-wpi coating on ti6al4v increases hydrophilicity and improves proliferation and differentiation of human bone marrow stromal cells,” *Int. J. Mol. Sci.*, vol. 23, no. 1, pp. 1–12, 2022, doi: 10.3390/ijms23010139.
- [9] Z. Hu *et al.*, “Scalable Milk-Derived Whey Protein Hydrogel as an Implantable Biomaterial,” *ACS Appl. Mater. Interfaces*, vol. 14, no. 25, pp. 28501–28513, 2022, doi: 10.1021/acsami.2c02361.
- [10] J. Yan *et al.*, “Formation, physicochemical properties, and comparison of heat- and enzyme-induced whey protein-gelatin composite hydrogels,” *Food Hydrocoll.*, vol. 137, no. December 2022, p. 108384, 2023, doi: 10.1016/j.foodhyd.2022.108384.
- [11] M. Dziadek *et al.*, “Novel multicomponent organic–inorganic WPI/gelatin/CaP hydrogel composites for bone tissue engineering,” *J. Biomed. Mater. Res. - Part A*, vol. 107, no. 11, pp. 2479–2491, 2019, doi: 10.1002/jbm.a.36754.
- [12] D. K. Baines *et al.*, “The Enrichment of Whey Protein Isolate Hydrogels with Poly- $\gamma$ -Glutamic Acid Promotes the Proliferation and Osteogenic Differentiation of Preosteoblasts,” *Gels*, vol. 10, no. 1, 2024, doi: 10.3390/gels10010018.
- [13] V. Platania, T. E. L. Douglas, M. K. Zubko, D. Ward, K. Pietryga, and M. Chatzinikolaidou, “Phloroglucinol-enhanced whey protein isolate hydrogels with antimicrobial activity for tissue engineering,” *Mater. Sci. Eng. C*, vol. 129, no. April, p. 112412, 2021, doi: 10.1016/j.msec.2021.112412.
- [14] V. O. Plastun *et al.*, “WPI Hydrogels with a Prolonged Drug-Release Profile for Antimicrobial Therapy,” *Pharmaceutics*, vol. 14, no. 6, pp. 1–15, 2022, doi: 10.3390/pharmaceutics14061199.
- [15] K. Norris *et al.*, “Marine-inspired enzymatic mineralization of dairy-derived whey protein isolate (WPI) hydrogels for bone tissue regeneration,” *Mar. Drugs*, vol. 18, no.

- 6, 2020, doi: 10.3390/md18060294.
- [16] J. Hogwood, B. Mulloy, R. Lever, E. Gray, and C. P. Page, "Pharmacology of Heparin and Related Drugs: An Update," *Pharmacol. Rev.*, vol. 75, no. 2, pp. 328–379, 2023, doi: 10.1124/pharmrev.122.000684.
- [17] E. I. Oduah, R. J. Linhardt, and S. T. Sharfstein, "Heparin: Past, present, and future," *Pharmaceuticals*, vol. 9, no. 3, pp. 1–12, 2016, doi: 10.3390/ph9030038.
- [18] Y. Liang and K. L. Kiick, "Heparin-functionalized polymeric biomaterials in tissue engineering and drug delivery applications," *Acta Biomater.*, vol. 10, no. 4, pp. 1588–1600, 2014, doi: 10.1016/j.actbio.2013.07.031.
- [19] A. M. Ferreira, P. Gentile, S. Toumpaniari, G. Ciardelli, and M. A. Birch, "Impact of Collagen/Heparin Multilayers for Regulating Bone Cellular Functions," *ACS Appl. Mater. Interfaces*, vol. 8, no. 44, pp. 29923–29932, 2016, doi: 10.1021/acsami.6b09241.
- [20] D. L. Rabenstein, "Heparin and heparan sulfate: Structure and function," *Nat. Prod. Rep.*, vol. 19, no. 3, pp. 312–331, 2002, doi: 10.1039/b100916h.
- [21] R. Manjunathan, K. Mitra, R. Vasvani, and M. Doble, "High molecular weight heparin-induced angiogenesis mainly mediated via basic fibroblast growth factor-2- an in-vivo (CAM) and in-silico analysis," *Biochem. Biophys. Reports*, vol. 37, no. December 2023, p. 101609, 2024, doi: 10.1016/j.bbrep.2023.101609.
- [22] J. H. Ahire *et al.*, "Polyurethane infused with heparin capped silver nanoparticles dressing for wound healing application: Synthesis, characterization and antimicrobial studies," *Int. J. Biol. Macromol.*, vol. 282, no. P1, p. 136557, 2024, doi: 10.1016/j.ijbiomac.2024.136557.
- [23] B. Sayed, D. M. Seoudi, and A. N. Badawi, "Chitosan / Heparin Complex As Efficient Strategy to Enhance Diabetic Wound Healing," *Egypt. J. Pure Appl. Sci.*, vol. 63, no. 1, pp. 1–12, 2025, doi: 10.21608/ejaps.2025.324838.1110.
- [24] H. T. Liao, Y. T. Lai, C. Y. Kuo, and J. P. Chen, "A bioactive multi-functional heparin-grafted aligned poly(lactide-co-glycolide)/curcumin nanofiber membrane to accelerate diabetic wound healing," *Mater. Sci. Eng. C*, vol. 120, no. November 2020, p. 111689, 2021, doi: 10.1016/j.msec.2020.111689.

- [25] K. Kohyama *et al.*, “Concomitant heparin use promotes skin graft donor site healing by basic fibroblast growth factor: A pilot prospective randomized controlled study,” *Contemp. Clin. Trials Commun.*, vol. 42, no. September, p. 101375, 2024, doi: 10.1016/j.conctc.2024.101375.
- [26] C. J. Yadav, U. Yadav, S. Afrin, J. Y. Lee, J. Kamel, and K. M. Park, “Heparin Immobilization Enhances Hemocompatibility, Re-Endothelization, and Angiogenesis of Decellularized Liver Scaffolds,” *Int. J. Mol. Sci.*, vol. 25, no. 22, 2024, doi: 10.3390/ijms252212132.
- [27] E. A. Nutescu, N. L. Shapiro, H. Feinstein, and C. W. Rivers, “Tinzaparin: Considerations for Use in Clinical Practice,” *Ann. Pharmacother.*, vol. 37, no. 12, pp. 1831–1840, 2003, doi: 10.1345/aph.1D221.
- [28] I. A. Vathiotis, N. K. Syrigos, and E. P. Dimakakos, “Tinzaparin Safety in Patients With Cancer and Renal Impairment: A Systematic Review,” *Clin. Appl. Thromb.*, vol. 27, pp. 4–10, 2021, doi: 10.1177/1076029620979592.
- [29] M. Amerali and M. Politou, “Tinzaparin—a review of its molecular profile, pharmacology, special properties, and clinical uses,” *Eur. J. Clin. Pharmacol.*, vol. 78, no. 10, pp. 1555–1565, 2022, doi: 10.1007/s00228-022-03365-4.
- [30] J. L. Neely, S. S. Carlson, and S. E. Lenhart, “Tinzaparin sodium: A low-molecular-weight heparin,” *Am. J. Heal. Pharm.*, vol. 59, no. 15, pp. 1426–1436, 2002, doi: 10.1093/ajhp/59.15.1426.
- [31] L. S. Litvinova *et al.*, “Osteogenic and Angiogenic Properties of Heparin as a System for Delivery of Biomolecules for Bone Bioengineering: a Brief Critical Review,” *Biochem. Suppl. Ser. B Biomed. Chem.*, vol. 15, no. 2, pp. 147–152, 2021, doi: 10.1134/S1990750821020050.
- [32] F. Zia, K. M. Zia, M. Zuber, S. Tabasum, and S. Rehman, “Heparin based polyurethanes: A state-of-the-art review,” *Int. J. Biol. Macromol.*, vol. 84, pp. 101–111, 2016, doi: 10.1016/j.ijbiomac.2015.12.004.
- [33] C. Hadjichristou *et al.*, “Biocompatibility assessment of resin-based cements on vascularized dentin/pulp tissue-engineered analogues,” *Dent. Mater.*, vol. 37, no. 5, pp. 914–927, 2021, doi: 10.1016/j.dental.2021.02.019.

- [34] J. Luzuriaga, J. Irurzun, I. Irastorza, F. Unda, G. Ibarretxe, and J. R. Pineda, "Vasculogenesis from human dental pulp stem cells grown in matrigel with fully defined serum-free culture media," *Biomedicines*, vol. 8, no. 11, pp. 1–19, 2020, doi: 10.3390/biomedicines8110483.
- [35] L. W. Bento *et al.*, "Endothelial differentiation of SHED requires MEK1/ERK signaling," *J. Dent. Res.*, vol. 92, no. 1, pp. 51–57, 2013, doi: 10.1177/0022034512466263.
- [36] O. Francesconi *et al.*, "Lipoyl-Based Antagonists of Transient Receptor Potential Cation A (TRPA1) Downregulate Osteosarcoma Cell Migration and Expression of Pro-Inflammatory Cytokines," *ACS Pharmacol. Transl. Sci.*, vol. 5, no. 11, pp. 1119–1127, 2022, doi: 10.1021/acspsci.2c00114.
- [37] F. Peyvandi, I. Garagiola, and L. Baronciani, "Role of von Willebrand factor in the haemostasis," *Blood Transfus.*, vol. 9, no. SUPPL. 2, pp. 3–8, 2011, doi: 10.2450/2011.002S.
- [38] S. Gengrinovitch *et al.*, "Platelet factor-4 inhibits the mitogenic activity of VEGF121 and VEGF165 using several concurrent mechanisms," *J. Biol. Chem.*, vol. 270, no. 25, pp. 15059–15065, 1995, doi: 10.1074/jbc.270.25.15059.
- [39] A. J. Devlin *et al.*, "Analysis of Heparin Samples by Attenuated Total Reflectance Fourier-Transform Infrared Spectroscopy in the Solid State," *ACS Cent. Sci.*, vol. 9, no. 3, pp. 381–392, 2023, doi: 10.1021/acscentsci.2c01176.
- [40] J. Devlin, "ATR-FTIR spectroscopy of heparin : using multivariate analyses for next-generation quality control.," 2023.
- [41] J. Zhu and R. E. Marchant, "Design properties of hydrogel tissue-engineering scaffolds," *Expert Rev. Med. Devices*, vol. 8, no. 5, pp. 607–626, 2011, doi: 10.1586/erd.11.27.
- [42] G. Janarthanan and I. Noh, "Recent trends in metal ion based hydrogel biomaterials for tissue engineering and other biomedical applications," *J. Mater. Sci. Technol.*, vol. 63, pp. 35–53, 2021, doi: 10.1016/j.jmst.2020.02.052.
- [43] H. Holback, Y. Yeo, and K. Park, *Hydrogel swelling behavior and its biomedical applications*. Woodhead Publishing Limited, 2011.

- [44] S. Bashir *et al.*, “Fundamental concepts of hydrogels: Synthesis, properties, and their applications,” *Polymers (Basel)*, vol. 12, no. 11, pp. 1–60, 2020, doi: 10.3390/polym12112702.
- [45] E. Budianto, S. P. Muthoharoh, and N. M. Nizardo, “Effect of Crosslinking Agents , pH and Temperature on Swelling Behavior of Cross - linked Chitosan Hydrogel,” *Asian J. Appl. Sci.*, vol. 03, no. 05, pp. 2321–893, 2015.
- [46] X. Jiang, C. L. Li, and Q. Han, “Modulation of swelling of PVA hydrogel by polymer and crosslinking agent concentration,” *Polym. Bull.*, vol. 80, no. 2, pp. 1303–1320, 2023, doi: 10.1007/s00289-022-04116-2.
- [47] H. Nasution *et al.*, “Hydrogel and Effects of Crosslinking Agent on Cellulose-Based Hydrogels: A Review,” *Gels*, vol. 8, no. 9, 2022, doi: 10.3390/gels8090568.
- [48] C. He *et al.*, “Heparin-based and heparin-inspired hydrogels: size-effect, gelation and biomedical applications,” *J. Mater. Chem. B*, vol. 7, no. 8, pp. 1186–1208, 2019, doi: 10.1039/c8tb02671h.
- [49] H. L. McRae, L. Militello, and M. A. Refaai, “Updates in anticoagulation therapy monitoring,” *Biomedicines*, vol. 9, no. 3, 2021, doi: 10.3390/biomedicines9030262.
- [50] R. Rajaraman, D. E. Rounds, S. P. S. Yen, and A. Rembaum, “A scanning electron microscope study of cell adhesion and spreading in vitro,” *Exp. Cell Res.*, vol. 88, no. 2, pp. 327–339, 1974, doi: 10.1016/0014-4827(74)90248-1.
- [51] B. E. Uygun, S. E. Stojasih, and H. W. T. Matthew, “Effects of immobilized glycosaminoglycans on the proliferation and differentiation of mesenchymal stem cells,” *Tissue Eng. - Part A*, vol. 15, no. 11, pp. 3499–3512, 2009, doi: 10.1089/ten.tea.2008.0405.
- [52] J. Ratanavaraporn and Y. Tabata, “Enhanced osteogenic activity of bone morphogenetic protein-2 by 2-O-desulfated heparin,” *Acta Biomater.*, vol. 8, no. 1, pp. 173–182, 2012, doi: 10.1016/j.actbio.2011.09.035.
- [53] K. Na *et al.*, “Heparin/poly(l-lysine) nanoparticle-coated polymeric microspheres for stem-cell therapy,” *J. Am. Chem. Soc.*, vol. 129, no. 18, pp. 5788–5789, 2007, doi: 10.1021/ja067707r.
- [54] D. S. W. Benoit, A. R. Durney, and K. S. Anseth, “The effect of heparin-functionalized

- PEG hydrogels on three-dimensional human mesenchymal stem cell osteogenic differentiation,” *Biomaterials*, vol. 28, no. 1, pp. 66–77, 2007, doi: 10.1016/j.biomaterials.2006.08.033.
- [55] C. S. Abhinand, R. Raju, S. J. Soumya, P. S. Arya, and P. R. Sudhakaran, “VEGF-A/VEGFR2 signaling network in endothelial cells relevant to angiogenesis,” *J. Cell Commun. Signal.*, vol. 10, no. 4, pp. 347–354, 2016, doi: 10.1007/s12079-016-0352-8.
- [56] N.d., “Heparin: Uses, Interactions, Mechanism of Action,” *DrugBank Online*. <https://go.drugbank.com/drugs/DB01109>.
- [57] A. Fletcher, “Haematology.,” *J. R. Army Med. Corps*, vol. 152, no. 4, pp. 250–265, 2006, doi: 10.1136/jramc-152-04-12.
- [58] C. Spadaccio *et al.*, “Heparin-releasing scaffold for stem cells: A differentiating device for vascular aims,” *Regen. Med.*, vol. 5, no. 4, pp. 645–657, 2010, doi: 10.2217/rme.10.25.
- [59] Y. Folkman, J., Shing, “Control of Angiogenesis by Heparin and Other Sulfated Polysaccharides,” *Adv. Exp. Med. Biol.*, vol. 313, pp. 355–364, 1992, doi: [https://doi.org/10.1007/978-1-4899-2444-5\\_34](https://doi.org/10.1007/978-1-4899-2444-5_34).
- [60] C. Wang *et al.*, “Engineering a vascular endothelial growth factor 165-binding heparan sulfate for vascular therapy,” *Biomaterials*, vol. 35, no. 25, pp. 6776–6786, 2014, doi: 10.1016/j.biomaterials.2014.04.084.
- [61] M. R. M. Presta, D. Leali, H. Stabile, R. Ronca, M. Camozzi, L. Coco, E. Moroni, S. Liekens, “Heparin derivatives as angiogenesis inhibitors,” *Curr. Pharm. Des.*, vol. 9, pp. 553–566, 2003, doi: <https://doi.org/10.2174/1381612033391379>.
- [62] K. Norrby and P. Østergaard, “Basic-Fibroblast-Growth-Factor-Mediated de novo Angiogenesis Is More Effectively Suppressed by Low-Molecular-Weight than by High-Molecular-Weight Heparin,” *Int. J. Microcirc. Exp.*, vol. 16, no. 1, pp. 8–15, 1996, doi: 10.1159/000179145.
- [63] K. Norrby, “2.5 kDa and 5.0 kDa heparin fragments specifically inhibit microvessel sprouting and network formation in VEGF165-mediated mammalian angiogenesis,” *Int. J. Exp. Pathol.*, vol. 81, no. 3, pp. 191–198, 2000, doi: 10.1046/j.1365-2613.2000.00150.x.

- [64] A. A. Khorana, A. Sahni, O. D. Altland, and C. W. Francis, “Heparin Inhibition of Endothelial Cell Proliferation and Organization is Dependent on Molecular Weight,” *Arterioscler. Thromb. Vasc. Biol.*, vol. 23, no. 11, pp. 2110–2115, 2003, doi: 10.1161/01.ATV.0000090671.56682.D7.